Journal of Alloys and Compounds 489 (2010) 631–637

Contents lists available at ScienceDirect

Journal of Alloys and Compounds

journal homepage: www.elsevier.com/locate/jallcom

Microstructural evolution of intermetallic compounds in Sn–3.5Ag–X (X = 0, 0.75Ni, 1.0Zn and 1.5In)/Cu solder joints during liquid aging

Jie Chen, Jun Shen*, Shiqiang Lai, Dong Min, Xiaochuan Wang

Department of Material Science and Engineering, Chongqing University, Chongqing 400044, China

ARTICLE INFO

Article history:
Received 22 June 2009
Received in revised form
21 September 2009
Accepted 22 September 2009
Available online 30 September 2009

Keywords:
Lead-free solder
Microstructure
Interfacial reaction
Intermetallic compound

ABSTRACT

In this paper, the microstructural evolution of IMCs in Sn–3.5Ag–X (X = 0, 0.75Ni, 1.0Zn, 1.5In)/Cu solder joints and their growth mechanisms during liquid aging were investigated by microstructural observations and phase analysis. The results show that two-phase (Ni_3Sn_4 and Cu_6Sn) IMC layers formed in Sn–3.5Ag–0.75Ni/Cu solder joints during their initial liquid aging stage (in the first 8 min). While after a long period of liquid aging, due to the phase transformation of the IMC layer (from Ni_3Sn_4 and Cu_6Sn phases to a $(Cu, Ni)_6Sn_5$ phase), the rate of growth of the IMC layer in Sn–3.5Ag–0.75Ni/Cu solder joints decreased. The two Cu_6Sn_5 and Cu_5Zn_8 phases formed in Sn–3.5Ag–1.0Zn/Cu solder joints during the initial liquid aging stage and the rate of growth of the IMC layers is close to that of the IMC layer in Sn–3.5Ag/Cu solder joints. However, the phase transformation of the two phases into a Cu–Zn–Sn phase speeded up the growth of the IMC layer. The addition of In to Sn–3.5Ag solder alloy resulted in $Cu_6(Sn_x,In_{1-x})_5$ phase which speeded up the growth of the IMC layer in Sn–3.5Ag–1.5In/Cu solder joint.

1. Introduction

Tin–lead solder has been widely used in the microelectronic packaging industry. However, increased environmental and health concerns over the toxicity of Pb in eutectic tin–lead solder and the sustained trend towards miniaturization and functional density enhancement of interconnections in microelectronic packaging have promoted the development of new lead-free solders for microelectronic packaging [1,2]. Generally, these lead-free solders are Sn-based binary and ternary alloys. Among these various lead-free solders, Sn–Ag solder is one of the most recommended candidates to replace Sn–Pb eutectic solder [3]. The Sn–Ag alloy is superior to Sn–Pb in terms of ductility, creep resistance and thermal resistance but has a higher melting point (the melting points of the eutectic Sn–Ag and Sn–Pb alloys are 494 K and 456 K respectively [4]) and poor wettability [5,6]. This relatively high melting point and poor wettability are considered as serious drawbacks of Sn–Ag solder in the microelectronics industry [7]. In order to solve these drawbacks, alloying elements have been added into Sn–Ag alloy to reduce its melting point and to improve the wettability. For example, the addition of minor amounts of Ni into the Sn–Ag alloy increased the wettability of the solder alloy and formed additional intermetallic phases, which improved the mechanical properties of solder joints [8]. In addition, the addition of minor amounts of Zn and In into Sn–3.5Ag solder alloy reduced their melting point (the melting points of Sn–3.5Ag–1.0Zn and Sn–3.5Ag–1.5In alloys are 490 K and 483.9 K respectively) [9,10].

The interfacial reactions between Sn–Ag–X solder alloys and substrates have also been studied. Liu et al. [11] reported about the phase evolution of the metastable Cu_5Zn_8 phase in a soldered Sn–3.7Ag–0.9Zn/Cu interface. After soldering for 1 min, the metastable Cu_5Zn_8 phase formed primarily. Then, part of the formed Cu_5Zn_8 layer changed into a stable Cu_6Sn_5 phase (close to the Cu plate). Kim et al. [12] studied the effects of additions of fourth alloying elements on the microstructures of Sn–3Ag–0.5Cu–X alloy solders and their joints with Cu. It was found that a flat and fine Sn–Cu–Ni IMC layer formed at Sn–3Ag–0.5Cu–0.1Ni/Cu joints. Lee and Lee [8] investigated the shear strength and interfacial microstructure of Sn–3.5Ag–*x*Ni/Cu single shear lap solder joints. In as-reflowed condition, only a $(Cu,Ni)_6Sn_5$ layer formed at the interface of Sn–Ag–*x*Ni/Cu and the thickness of the IMC layer increased with an increase of the Ni content. However, the effect of the increased IMC layer thickness following the thermal storage does not appear to have a significant effect on the shear strength of the joint. Sharif and Chan [13] studied liquid and solid interfacial reactions between a Sn–3.5Ag–9In–0.5Cu solder and a Ni–P under bump metallization. The presence of indium in the solder played a major role in inhibiting the consumption of Ni(P) in the soldering reaction. A stable $(Cu,Ni)_6$ $(Sn,In)_5$ IMC initially formed at the interface of the Ni(P)/In-containing solder system. During further reflow, $(Cu, Ni)_3(Sn, In)_4$ IMCs started forming because of the limited Cu content in the solder.

* Corresponding author. Tel.: +86 23 13883111150; fax: +86 23 67084927.
E-mail address: shenjun2626@163.com (J. Shen).

0925-8388/$ – see front matter © 2009 Elsevier B.V. All rights reserved.
doi:10.1016/j.jallcom.2009.09.135

The research mentioned above focused on the melting point, wettability and the interfacial reaction between Sn–Ag–X solders and substrates. In microelectronic devices, because solder joints work in a high-temperature environment due to the Joule heating of devices, in particular, solder joints may be partially melted and this will degrade both the mechanical properties of solder joints and the life-time of devices. Hence, in this study, four solder alloys (Sn–3.5Ag–X (X = 0, 0.75Ni, 1.0Zn, 1.5In)) were used for liquid aging tests to investigate the microstructural evolution of IMCs in Sn–3.5Ag–X/Cu joints. The reason of using 0.75Ni, 1.0Zn and 1.5In in the alloys is that they are near eutectic composition (with lower melting temperatures) and these alloys are/will be used in industry system. In the following description, we name Sn–3.5Ag as Sn–Ag, Sn–3.5Ag–0.75Ni as Sn–Ag–Ni, Sn–3.5Ag–0.1Zn as Sn–Ag–Zn and Sn–3.5Ag–0.5In as Sn–Ag–In. In addition, the growth mechanisms of IMCs were also investigated in detail.

2. Experimental procedures

Sn–3.5Ag, Sn–3.5Ag–0.75Ni, Sn–3.5Ag–1.5In and Sn–3.5Ag–1.0Zn solder alloys were prepared from bulk rods of pure Sn, Ag, Ni, In and Zn. After weighing the individual pure metals, they were mixed and melted in a vacuum arc furnace under a high purity argon atmosphere to produce button-like specimens with a diameter of about 35 mm. In order to get a homogeneous composition, all ingots were remelted five times. Finally they were solidified in a water-cooled copper mould with a cooling rate of about 20 K s^{-1}. The experimental substrates were 99.99% purity Cu plates with 15 mm length, 7 mm width and 6 mm thickness. They were polished with diamond powders and degreased in ethanol (with 1 vol.% HCl) so as to remove surface oxides and impurities. Sn–Ag–X (0, Ni, Zn, In) lead-free solders were placed on the Cu plates to be manually soldered at a temperature of 550–600 K for about 1 min. After manual soldering, the solder specimens were placed in a heated furnace (SX2-4-10) quickly and liquid aged at a temperature of 583 K corresponding with the temperature of manual soldering for 8 min, 24 min and 40 min in ambient air [14,15]. Then, the samples were cooled down to room temperature in the air ambient.

Cross-sections of the solders/Cu interfaces were prepared by standard metallographic procedures (grinding, polishing and etching with a solution of 5 vol.% HNO_3 + 92 vol.% C_2H_5OH + 3 vol.% HCl). The microstructures of solder joints were characterized by scanning electron microscopy (TESCAN, Inc. VegaIILMU SEM). Energy dispersive spectroscopy X-ray (OXFORD, Inc., ISIS300 EDS) analysis was performed to identify the IMCs phases.

The average thickness of the IMC layers (x) in the as-soldered solder joints was determined by element distribution line scanning maps. While, the average thickness of the IMC layers (x) in liquid aged solder joints were calculated through dividing the integrated area by the length of the IMC layers.

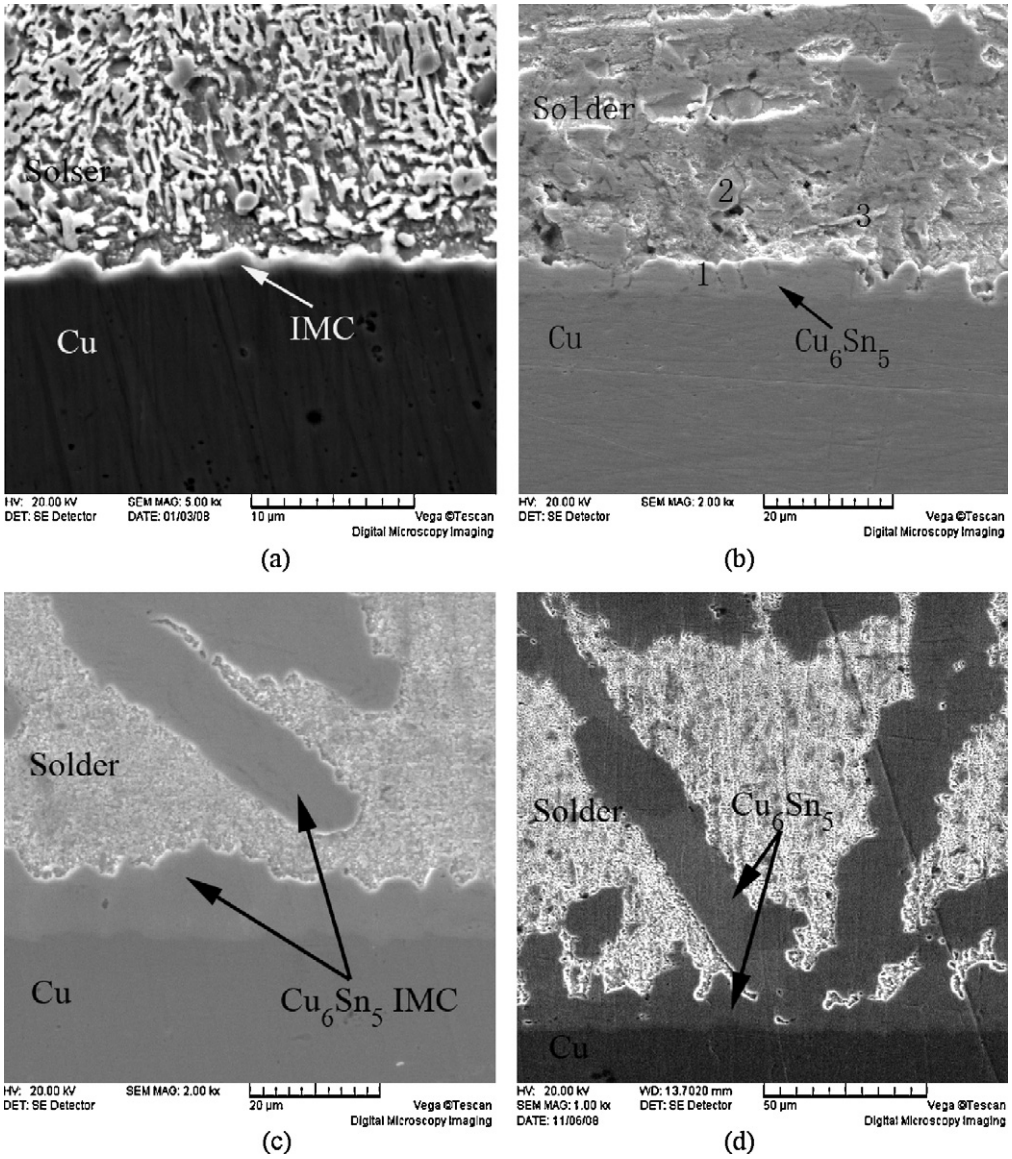

Fig. 1. The microstructural evolution of Sn–Ag/Cu solder joints, (a) manually soldered for 1 min, (b) liquid aged for 8 min, (c) liquid aged for 24 min and (d) liquid aged for 40 min.

3. Results and discussion

3.1. Microstructural evolution of IMCs

3.1.1. The microstructural evolution of IMCs in Sn–Ag/Cu solder joints

Fig. 1 shows the microstructural evolution of IMCs in Sn–Ag/Cu joints during liquid aging. It can be seen from Fig. 1(a) that, after manual soldering, a uniform and continuous IMC layer formed between the Sn–Ag solder alloy and the Cu substrate. According to Laurila et al. [16], it was believed that the IMC layer was composed of Cu_6Sn_5 particles (thickness of this layer was ~2 μm). After liquid aging for 8 min, scallop-like Cu_6Sn_5 particles with an average thickness of ~5.5 μm grew towards the solder matrix (as shown in Fig. 1(b)). It can be noticed that some of the Cu_6Sn_5 particles were separated from the IMC layer, and were embedded in the solder matrix (EDS analysis (see Table 1) shows the atomic percentage of Cu and Sn at point 1 was about 6:5). After the specimens were aged for 24 min (see Fig. 1(c)), the average thickness of this Cu_6Sn_5 interfacial layer was about 9.5 μm. However, more Cu_6Sn_5 particles were seen to be separated from the main IMC layer and embedded in the solder matrix. This is because during the liquid aging, Cu_6Sn_5 particles were dissolved from the IMC layer into the molten solder through both grain boundaries and grain surfaces which were in contact with the molten solder, as long as the molten solder remained unsaturated with Cu [17]. After liquid aging for 40 min (see Fig. 1(d)), the Cu_6Sn_5 layer became thicker (with an average thickness of ~22 μm). However, more dissolved Cu combined with Sn atoms to form bulk Cu_6Sn_5 particles and accumulate together in the solder matrix inhomogeneously during solidification. According to Ref. [18], the IMCs in solder matrix formed by solidification

Table 1
EDS chemical analysis of Sn–Ag/Cu joint aging at 523 K for 8 min.

Element	Point					
	1		2		3	
	wt%	at%	wt%	at%	wt%	at%
Sn	63.53	48.25	64.17	48.95	95.44	94.31
Cu	36.47	51.75	35.83	51.05	0.97	1.79
Ag	0	0	0	0	3.59	3.91

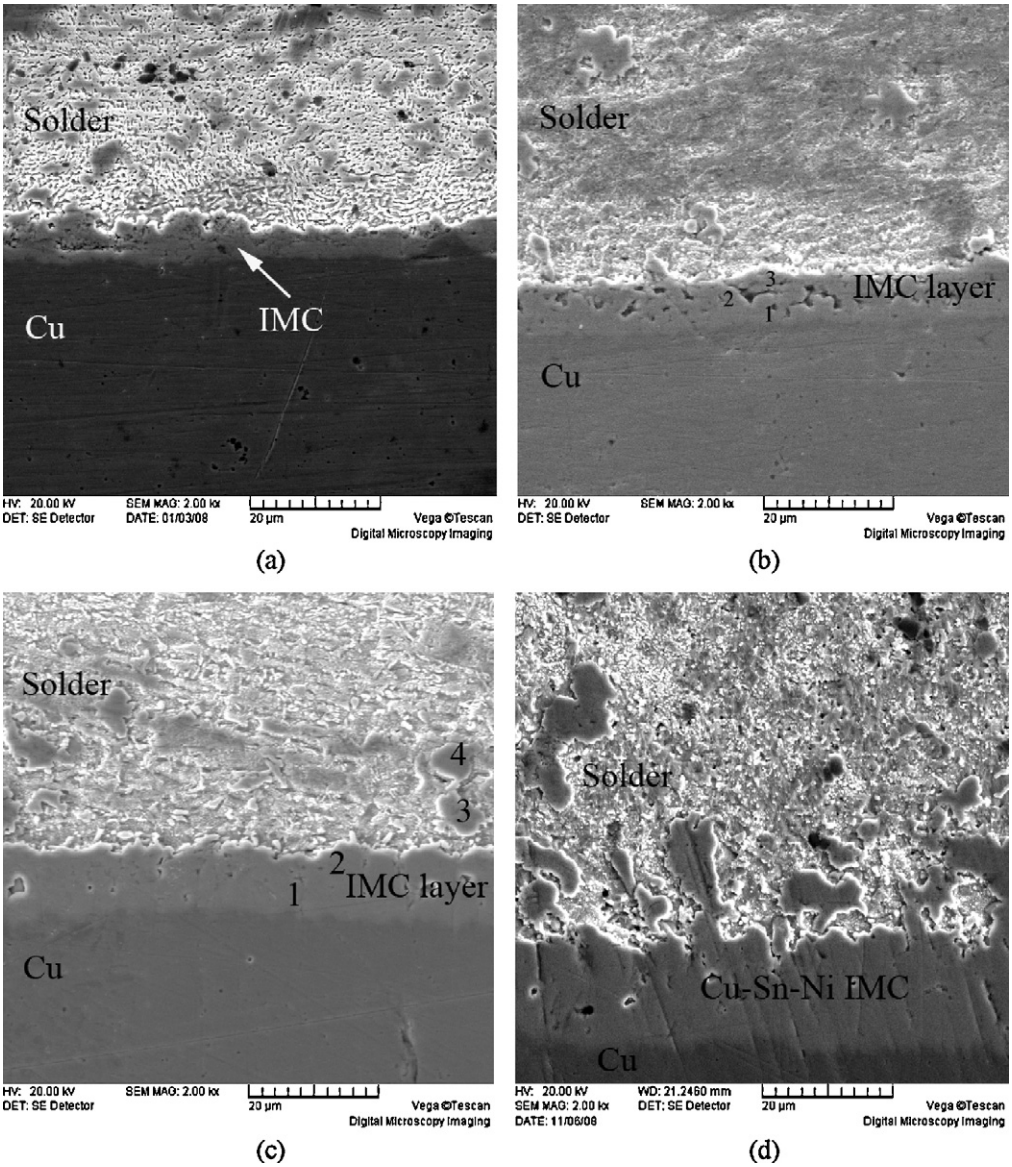

Fig. 2. The microstructural evolution of Sn–Ag–Ni/Cu solder joints, (a) manually soldered for 1 min, (b) liquid aged for 8 min, (c) liquid aged for 24 min and (d) liquid aged for 40 min.

Table 2
EDS chemical analysis of Sn–Ag–Ni/Cu joint aging at 523 K for 8 min.

Element	Point					
	1		2		3	
	Wt%	At%	Wt%	At%	Wt%	At%
Sn	56.02	40.49	73.59	59.69	78.34	65.68
Ni	1.29	1.89	2.42	3.97	3.19	5.41
Cu	42.68	57.62	23.98	36.34	18.46	28.91

usually have faceted structure. Due to the inherently brittle nature of IMC layers and their tendency to generate structural defects, such structure of bulk Cu_6Sn_5 IMC may degrade the fatigue and fracture strengths of solder joints, leading to poor reliability of electronic devices.

3.1.2. The microstructural evolution of IMCs in Sn–Ag–Ni/Cu solder joints

For both the manually soldered and liquid aged samples of 8 min, the IMC layers formed in Sn–Ag–Ni/Cu solder joints with average thicknesses of ~7 μm and ~9 μm, respectively (see Fig. 2(a) and (b)). It is interesting that the IMC layer in Fig. 2(b) was more flat than that in Fig. 1(b). The EDS analysis results (shown in Table 2) show that the content of Ni in the IMCs layer reduces in the direction from the solder alloy to the Cu substrate. Hence, this proves that the Cu–Sn phases mainly located at the lower side of the IMC layer, while the Ni–Sn phases mainly formed at the upper side of the IMC layer. According to Chen et al. [19], it is certain that the IMCs layer were composed of Cu_6Sn_5 particles (close to the Cu substrate) and Ni_3Sn_4 particles (close to the solder matrix).

Compared with the interface between the IMC layers and solder matrix in Sn–Ag/Cu solder joints, the interface between IMC (Cu_6Sn_5 phase and Ni_3Sn_4 phase) layer and the Sn–Ag–Ni solder matrix is flattened due to minor Ni addition. When the liquid solder wets the Cu substrate, Cu_6Sn_5 phases are formed at the interface due to diffusion of atoms. During the consequent cooling process, since the rate of nucleation on the concave surface of grooves is highest (a heterogeneous nucleation mechanism), Ni_3Sn_4 particles in the liquid solder prefer to nucleate and easily grow in the grooves of the scallop-like Cu_6Sn_5 particles to form a flat surface on the IMC layer [20]. According to the EDS result (see Table 3), the IMC layer after 24 min liquid aging was still composed of Cu, Ni and Sn. However, there is no obvious difference in content of each element in different parts of the IMC layer. Hence, it is clear that the IMC layer changed into a homogeneous single-phase layer with a thickness of about 12 μm (see Fig. 2(c)). Previously, Lee and Lee [8] and Wang and Kao [21] reported that this IMC layer is composed of the $(Cu, Ni)_6Sn_5$ phase. Since both of Cu and Ni have a similar FCC lattice structure and similar atomic sizes, the substitution of Ni into Cu_6Sn_5 is to be expected without causing lattice distortion or the formation of a new phase [22]. After aging for 40 min, the thickness of the whole IMC layer increased to about 19 μm (see Fig. 2(d)).

Table 3
EDS chemical analysis of Sn–Ag–Ni/Cu joint aging at 523 K for 24 min.

Element	Point							
	1		2		3		4	
	Wt%	At%	Wt%	At%	Wt%	At%	Wt%	At%
Sn	78.90	66.55	66.37	51.17	66.00	50.26	65.48	49.65
Ni	1.53	2.61	3.34	5.21	11.70	18.01	12.49	19.14
Cu	19.57	30.84	30.29	43.62	22.30	31.73	22.03	31.21

3.1.3. The microstructural evolution of IMCs in Sn–Ag–Zn/Cu solder joints

After manual soldering, a thin IMC layer (with an average thickness of about 3.5 μm) formed in Sn–Ag–Zn/Cu solder joints (see Fig. 3(a)). However, Fig. 3(b) shows that two IMC layers (the average thickness of the IMC layers is about ~6 μm) formed at the interface of the solder joint consisting of a flat IMC layer on the bottom and a scallop-like IMC layer above it. Liu et al. [11] stated that due to the decomposition of Cu_5Zn_8 layer, these two IMC layers were composed of a Cu_6Sn_5 layer (close to the Cu substrate) and a Cu_5Zn_8 layer (close to the solder alloy). However, results from EDS measurements in Fig. 3(b) indicates that the present of Zn near the Cu substrate (see Fig. 3(e)). Therefore, it can be confirmed that the IMC layer formed close to the Cu substrate was the Cu_5Zn_8 phase while the scallop-like IMC layer close to solder matrix should be the Cu_6Sn_5 phase. This conclusion can also be supported by a thermodynamic analysis. The Gibbs free energy of formation (ΔG) of the Cu_5Zn_8 phase (−12.34 kJ/mol) is much lower than that of the Cu_6Sn_5 phase (−7.42 kJ/mol) [23]. Hence, Zn atoms are more reactive than Sn atoms with Cu atoms and the Cu_5Zn_8 phase should be the phase which formed first near to the Cu substrate. The discrepancy on the interfacial productions between ours and Ref. [11] can be attributed to the different alloy composition and soldering process. So the Cu_5Zn_8 layer did not decompose during the initial stage aging. Interestingly, after liquid aging for 24 min, the boundary between the Cu_6Sn_5 layer and the Cu_5Zn_8 layer disappeared and only one layer can be observed at the interface with an average thickness of ~15 μm (see Fig. 3(c)). This is because the Cu–Zn IMCs becomes unstable at temperatures as high as 150 °C [24]. After high-temperature aging, the metastable Cu_5Zn_8 IMC decomposes into Zn and Cu atoms and the Cu atoms combine with Sn atoms to form a stable Cu_6Sn_5 IMC layer with minor amount of Zn dissolved in it [11]. Hence, after liquid aging for 40 min, only a coarse Cu–Zn–Sn layer formed in Sn–Ag–Zn/Cu solder joints with an average thickness of ~27 μm (see Fig. 3(d)).

3.1.4. The microstructural evolution of IMCs in Sn–Ag–In/Cu solder joints

Fig. 4(a) shows that, after manual soldering, a very thin IMC layer (with an average thickness of about 2.5 μm) formed in Sn–Ag–In/Cu solder joints. After liquid aging for 8 min, the IMC particles were scallop-like and grew towards the solder matrix with an average thickness of ~5 μm (see Fig. 4(b)). Sharif and Chan [25] established that the composition of IMCs in Sn–3.5Ag–9In–0.5Cu/Cu joints are $Cu_{54.5}Sn_{42.7}In_{2.8}$, which corresponds to a $Cu_6(Sn_x,In_{1-x})_5$ phase. In this study, only a small addition of indium (1.5%) was made to the Sn–Ag solder alloy and the IMCs formed in Sn–Ag–In/Cu solder joints would be a $Cu_6(Sn,In_{minor})_5$ phase, which contained minor amount of indium. EDS analysis results show that after liquid aging for 24 min and 40 min, the phase of the IMC layer in Sn–Ag–In/Cu solder joints did not change while the average thicknesses of them were ~15 μm and ~19 μm, respectively (see Fig. 4(c) and (d)).

3.2. Growth mechanism

The microstructural observations given above indicate that the microstructures and phases of IMC layers in Sn–Ag–X/Cu solder joints changed during long term liquid aging (the phase evolution of IMCs are summarized in Table 4). In order to clarify the growth mechanism of the IMC layers between the four types of solder joints, the average thickness of the IMC layers in each solder joint against the liquid aging time are given in Fig. 5. It can be seen that the thickness of the IMC layers in each solder joint increased with an increase of the aging time, but the rates of growth were different. The rate of growth of the IMC layer in Sn–Ag–Ni/Cu solder joints was faster than that in Sn–Ag/Cu solder joints during the first

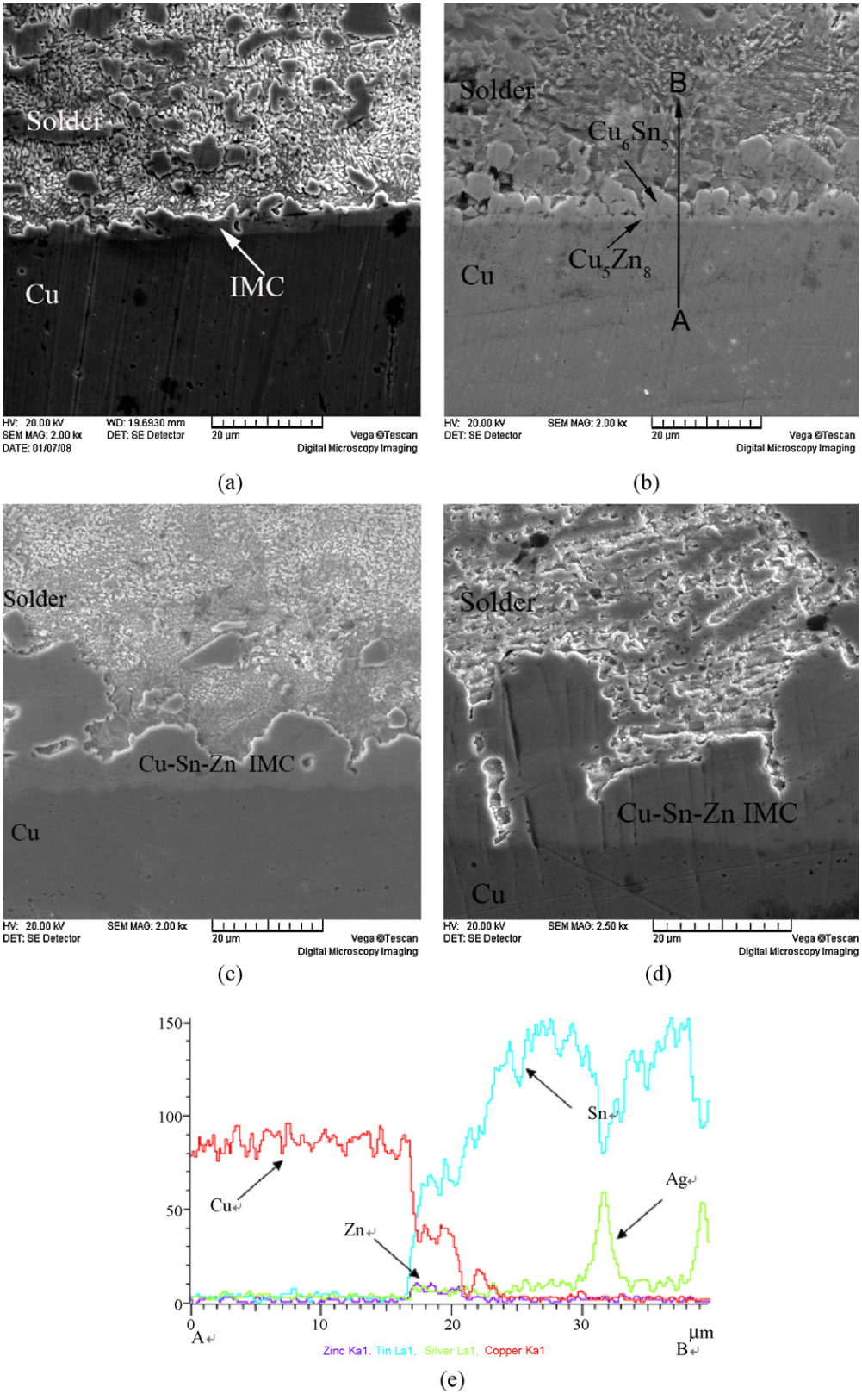

Fig. 3. The microstructural evolution of Sn–Ag–Zn/Cu solder joints, (a) manually soldered for 1 min, (b) liquid aged for 8 min, (c) liquid aged for 24 min, (d) liquid aged for 40 min and (e) the elemental distribution curves of a solder joint for (b) after liquid aging for 8 min.

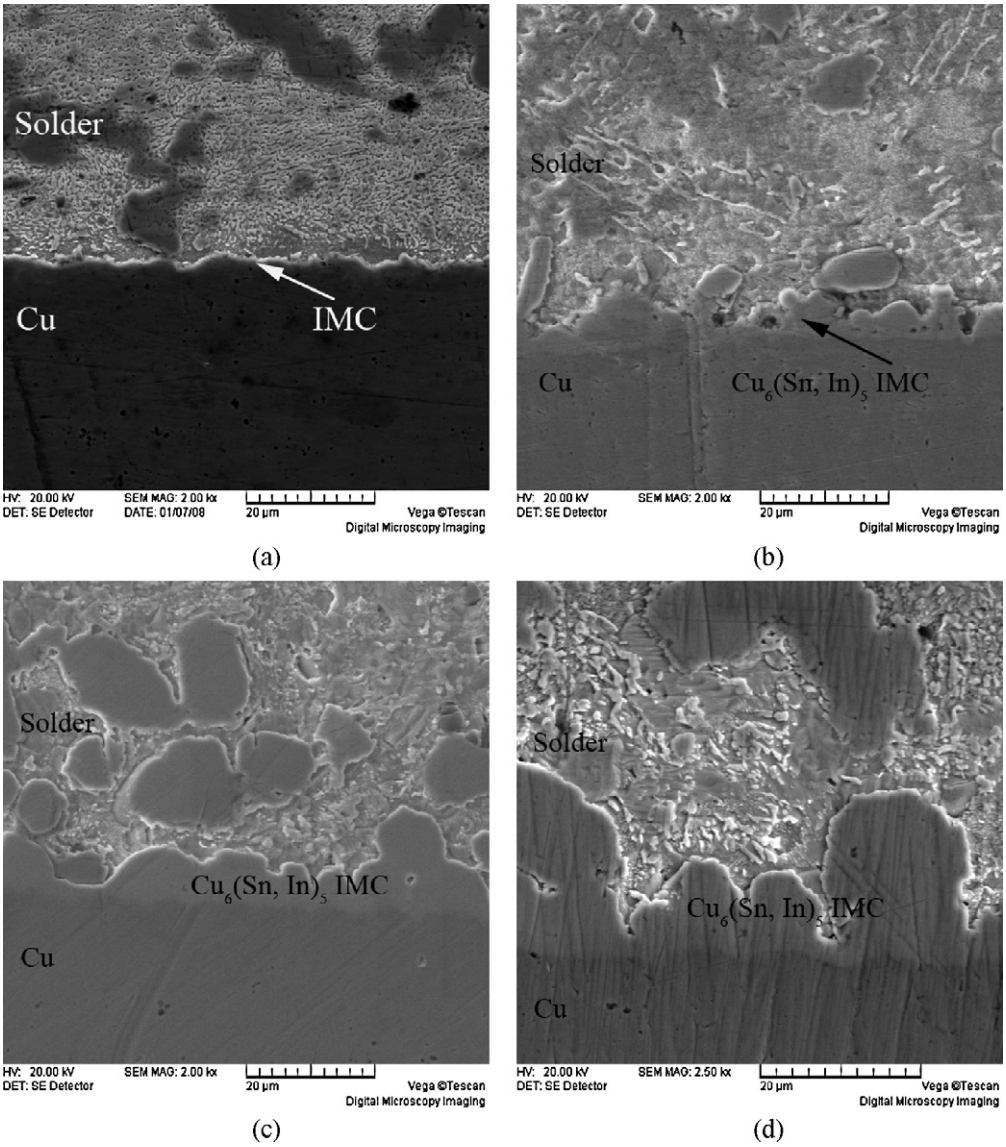

Fig. 4. The microstructural evolution of Sn–Ag–In/Cu solder joints, (a) manually soldered for 1 min, (b) liquid aged for 8 min, (c) liquid aged for 24 min and (d) liquid aged for 40 min.

8 min aging due to the heterogeneous nucleation and growth of the Ni_3Sn_4 phase in the grooves of the scallop-like Cu_6Sn_5 phase which enhanced the thickening of the IMC layer in Sn–Ag–Ni/Cu solder joints. However, after aging for 24 min, when the $(Cu,Ni)_6Sn_5$ phase were formed in Sn–Ag–Ni/Cu solder joints, the rate of growth of the $(Cu,Ni)_6Sn_5$ IMC layer decreased because, the diffusion of Cu was restrained due to the migration of Ni. Hence, after aging for 40 min, the average thickness of the IMC layer in Sn–Ag–Ni/Cu solder joints is thinner than that of Sn–Ag/Cu solder joints.

With 24 min aging, IMC layers which were composed of the Cu_5Zn_8 phase (an HCP structure) and the Cu_6Sn_5 phase (a FCC structure) formed in Sn–Ag–Zn/Cu solder joints. Since the atomic density of Cu_5Zn_8 (0.74) is close to that of Cu_6Sn_5 (0.68), the rates of growth of IMC layers formed in Sn–Ag/Cu solder joints and Sn–Ag–Zn/Cu solder joints are similar. However, after aging for 24 min, the metastable Cu_5Zn_8 phase decomposed and a Cu–Zn–Sn phase formed in the Sn–Ag–Zn/Cu solder joints. The Cu atoms from the decomposed Cu_5Zn_8 phase diffused towards the solder matrix and combined with Sn atoms to form additional Cu_6Sn_5 phase. As a result, the rate of growth of the IMC layer in Sn–Ag–Zn/Cu solder joints was faster than that of Sn–Ag/Cu solder joints and the average thickness of the Cu–Zn–Sn layer was thicker than that of the Cu_6Sn_5 layer in Sn–Ag/Cu solder joints.

No phase transformation of IMC layers occurred during aging of both Sn–Ag/Cu and Sn–Ag–In/Cu solder joints. However, the rate of growth of the IMC layer in Sn–Ag–In/Cu solder joints was faster than

Table 4
A summary of the phase evolution of IMCs in Sn–Ag–X (X = 0, Ni, Zn and In)/Cu solder joints.

Solder alloys	Manually soldered and liquid aged for 8 min	Liquid aged for 24 min	Liquid aged for 40 min
Sn–Ag/Cu	Cu_6Sn_5	Cu_6Sn_5	Cu_6Sn_5
Sn–Ag–Ni/Cu	Ni_3Sn/Cu_6Sn_5	$(Cu,Ni)_6Sn_5$	$(Cu,Ni)_6Sn_5$
Sn–Ag–Zn/Cu	Cu_6Sn_5/Cu_5Zn_8	Cu–Sn–Zn	Cu–Sn–Zn
Sn–Ag–In/Cu	$Cu_6(Sn,In_{minor})_5$	$Cu_6(Sn,In_{minor})_5$	$Cu_6(Sn,In_{minor})_5$

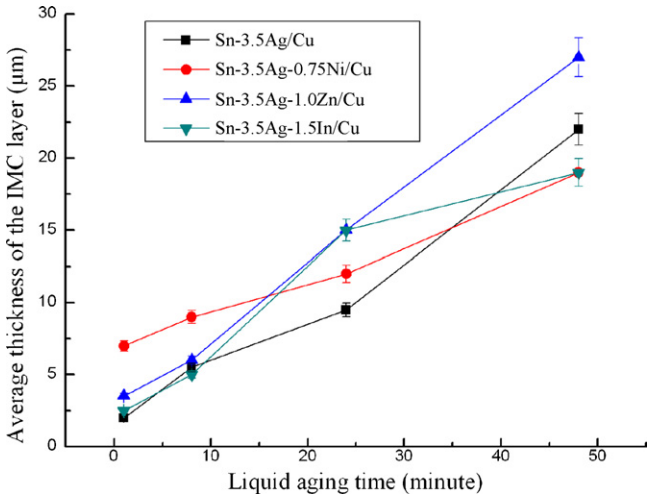

Fig. 5. The variations of the average thickness of IMC layers in each solder joint with the liquid aging time.

that in Sn–Ag/Cu solder joints during the middle stage of the liquid aging. This is because both In and Cu atoms took part in the interfacial reaction to form a $Cu_6(Sn_x,In_{1-x})_5$ IMC layer. However, after long term aging (i.e. 40 min), due to the exhaustion of the In contained in the Sn–Ag–In solder alloy due to the interfacial reaction, the rate of growth of the $Cu_6(Sn_x,In_{1-x})_5$ IMC layer in Sn–Ag–In/Cu solder joints was similar to that in Sn–Ag/Cu solder joints.

4. Conclusions

In this paper, the microstructural evolution of IMCs in Sn–Ag–X (X = 0, Ni, Zn, In)/Cu solder joints and their growth mechanisms during liquid aging were investigated and the conclusions may be summarized as follows:

(1) Compared with the growth of single IMC layer in Sn–Ag/Cu solder joints, there were two-phase (Ni_3Sn_4 and Cu_6Sn) IMC layers formed in Sn–Ag–Ni/Cu solder joints during their initial liquid aging stage (in the first 8 min). However, after long term aging (more than 24 min), the rate of growth of the IMC layer in Sn–Ag–Ni/Cu solder joints decreased due to the phase transformation (from two Ni_3Sn_4 and Cu_6Sn phases to a $(Cu, Ni)_6Sn_5$ phase).
(2) IMC layers with two Cu_6Sn_5 and Cu_5Zn_8 phases formed in Sn–Ag–Zn/Cu solder joints initially during the liquid aging and the rate of growth of these IMC layers were close to that of the layers in Sn–Ag/Cu solder joints. After long term liquid aging, IMC layers with two phases transformed into a Cu–Zn–Sn phase which speeded up its growth.
(3) The addition of In into the Sn–Ag solder alloy to form the $Cu_6(Sn_x,In_{1-x})_5$ phase speeded up the growth of the IMC layer in Sn–Ag–In/Cu solder joints until the indium became exhausted due to the interfacial reaction.

Acknowledgements

This research was financial supported by a Research Fund for the Doctoral Program of Higher Education of China (Project No. 20070611029) and Key Scientific and Technological Project of Chongqing (Project No. CSTC, 2009AC4046).

References

[1] K. Zeng, K.N. Tu, Mater. Sci. Eng. R 38 (2002) 55–105.
[2] F. Wang, M. O'Keefe, B. Brinkmeyer, J. Alloys Compd. 477 (2009) 267–273.
[3] J. Shen, Y.C. Liu, Y.J. Han, Y.M. Tian, H.X. Gao, J. Electron. Mater. 35 (2006) 1672–1679.
[4] J. Chen, J. Shen, D. Min, C. Peng, J. Mater. Sci. : Mater. Electron. 20 (2009) 1112–1117.
[5] I. Shohji, T. Yoshida, T. Takahashi, S. Hioki, Mater. Sci. Eng. A 366 (2004) 50–55.
[6] C.Y. Lin, J.H. Chou, Y.G. Lee, U.S. Mohanty, J. Alloys Compd. 470 (2009) 328–331.
[7] M. Abtew, G. Selvaduray, Mater. Sci. Eng. R 27 (2000) 95–141.
[8] Y.H. Lee, H.T. Lee, Mater. Sci. Eng. A 444 (2007) 75–83.
[9] J. Shen, S. Lai, Y. Liu, H. Gao, J. Wei, J. Mater. Sci.: Mater. Electron. 19 (2008) 275–280.
[10] M. McCormack, S. Jin, J. Electron. Mater. 23 (1994) 715–720.
[11] Y.C. Liu, J.B. Wan, Z.M. Gao, J. Alloys Compd. 465 (2008) 205–209.
[12] K.S. Kim, S.H. Huh, K. Suganuma, Microelectron. Reliab. 43 (2003) 259–267.
[13] A. Sharif, Y.C. Chan, Thin Solid Films 504 (2006) 431–435.
[14] J.F. Li, S.H. Mannan, M.P. Clode, D.C. Whalley, D.A. Hutt, Acta Mater. 54 (2006) 2907–2922.
[15] J.F. Li, S.H. Mannan, M.P. Clode, Scripta Mater. 54 (2006) 1773–2177.
[16] T. Laurila, V. Vuorinen, J.K. Kivilahti, Mater. Sci. Eng. R 49 (2005) 1–60.
[17] V.I. Dybkov, Growth Kinetics of Chemical Compound Layers, Cambridge International Science, Cambridge, 1998, pp. 135–136.
[18] J. Shen, Y.C. Chan, S.Y. Liu, Acta Mater. 57 (2009) 5196–5206.
[19] S.W. Chen, C.H. Wang, S.K. Lin, C.N. Chiu, J. Mater. Sci.: Mater. Electron. 18 (2007) 19–37.
[20] D.L. Shu, Metallic and Heat Treatment, Machine Industry, Beijing, 1983, pp. 45–46.
[21] Y.W. Wang, C.R. Kao, Microsystems, Packaging, Assembly and Circuits Technology, 2007. IMPACT 2007. International, October 1–3, 2007, pp. 280–283.
[22] P. Suna, C. Andersson, X. Wei, Z. Chen, D. Shangguan, J. Liu, J. Alloys Compd. 437 (2007) 169–179.
[23] M.-C. Wang, S.-P. Yu, T.-C. Chang, M.-H. Hon, J. Alloys Compd. 389 (2005) 133–140.
[24] K. Suganuma, K.S. Kim, J. Mater. Sci.: Mater. Electron. 18 (2007) 121–127.
[25] A. Sharif, Y.C. Chan, J. Alloys Compd. 390 (2005) 67–73.